AD-A074 502 STANFORD UNIV CA EDWARD L GINZTON LAB F/G 20/6
ACOUSTIC MICROSCOPY AT CRYOGENIC TEMPERATURES.(U)
SEP 79 C F QUATE, J HEISERMAN N00014-77-C-0412
UNCLASSIFIED GL-3008 NL

/ OF \
AD
A074502

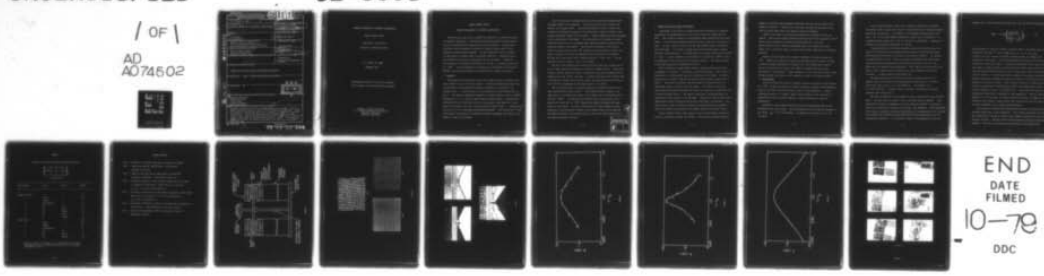

END
DATE
FILMED
10-79
DDC

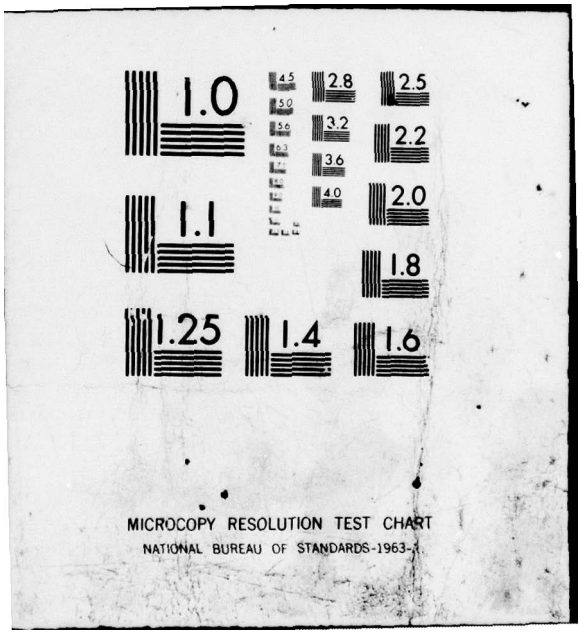
1.0
1.1
1.25
1.4
1.6
1.8
2.0
2.2
2.5
2.8
3.2
3.6
4.0
4.5
5.0
5.6
6.3
MICROCOPY RESOLUTION TEST CHART
NATIONAL BUREAU OF STANDARDS-1963-A

UNCLASSIFIED

SECURITY CLASSIFICATION OF THIS PAGE (When Data Entered)

(12) LEVEL II AD-E 391

REPORT DOCUMENTATION PAGE

READ INSTRUCTIONS BEFORE COMPLETING FORM

1. REPORT NUMBER: G.L. Report No. 3008
2. GOVT ACCESSION NO.
3. RECIPIENT'S CATALOG NUMBER (9)
4. TITLE (and Subtitle): (6) ACOUSTIC MICROSCOPY AT CRYOGENIC TEMPERATURES
5. TYPE OF REPORT & PERIOD COVERED: Annual Summary Report. 1 July 1978 — 30 June 1979
6. PERFORMING ORG. REPORT NUMBER: G.L. Report No. 3008
7. AUTHOR(s): (10) C. F. Quate, J. Heiserman
8. CONTRACT OR GRANT NUMBER(s): (15) N00014-77-C-0412
9. PERFORMING ORGANIZATION NAME AND ADDRESS: Edward L. Ginzton Laboratory, W. W. Hansen Laboratories of Physics, Stanford University, Stanford, Ca. 94305
10. PROGRAM ELEMENT, PROJECT, TASK AREA & WORK UNIT NUMBERS: Task NR 384-924
11. CONTROLLING OFFICE NAME AND ADDRESS: Office of Naval Research, Physics Program Office, Arlington, Virginia 22217
12. REPORT DATE: September 1979
13. NUMBER OF PAGES: 21 (12) 21 p.
14. MONITORING AGENCY NAME & ADDRESS (if different from Controlling Office): (14) GL-3008
15. SECURITY CLASS. (of this report): UNCLASSIFIED
15a. DECLASSIFICATION/DOWNGRADING SCHEDULE
16. DISTRIBUTION STATEMENT (of this Report)

"Approved for public release; distribution unlimited".

17. DISTRIBUTION STATEMENT (of the abstract entered in Block 20, if different from Report)
18. SUPPLEMENTARY NOTES

DDC RECEIVED OCT 1 1979 B

19. KEY WORDS (Continue on reverse side if necessary and identify by block number)

Acoustic microscopy
Superfluid helium
Liquid argon
Liquid nitrogen
Mechanical scanning

ANGSTROM degrees

20. ABSTRACT (Continue on reverse side if necessary and identify by block number)

We report progress in work on a cryogenic acoustic microscope. Results in liquid argon and nitrogen at about 4300 Å wavelength are discussed. Images of gratings and integrated circuits are presented as examples of resolution and contrast. Work on producing effective matching layers to improve acoustic power transfer between solids and helium is summarized. Finally we present images taken in superfluid helium held at 1.95°K. A wavelength of 3600 Å was attained, the shortest wavelength ever achieved in an acoustic microscope.

DD FORM 1 JAN 73 1473

UNCLASSIFIED

SECURITY CLASSIFICATION OF THIS PAGE (When Data Entered)

409 640

79 09 25 044

AD A074502

DDC FILE COPY

ACOUSTIC MICROSCOPY AT CRYOGENIC TEMPERATURES

Annual Summary Report

1 July 1978 - 30 June 1979

Contract No. N00014-77-C-0412

G. L. Report No. 3008

September 1979

Edward L. Ginzton Laboratory
W. W. Hansen Laboratories of Physics
Stanford University
Stanford, California

ANNUAL SUMMARY REPORT

"ACOUSTIC MICROSCOPY AT CRYOGENIC TEMPERATURES"

During the past year we have extended our experience in acoustic microscopy at cryogenic temperatures. The microscope has been operated in liquid argon at a level of resolution which surpasses the optical instrument. We have found that nearly equal performance is possible in liquid nitrogen, which is less expensive and more readily available. We have conducted a series of studies in liquid argon to evaluate areas of potential usefulness. Promising results were obtained in the areas of integrated circuits and biology. Finally we have succeeded in operating the microscope at 630 MHz in superfluid helium held at $1.95^{\circ}K$. At this temperature and frequency the wavelength in the liquid is 3600 $\mathring{A}$, the shortest wavelength ever achieved with an acoustic microscope.

1. Apparatus

The apparatus and electronics used in the cryogenic acoustic microscope were fully described in our first annual report.[1] Significant modifications have been recently made to the scanning device which has improved the stability of the scanning raster. A cross section of the new mechanism is shown schematically in Fig. 1. The sample is mounted horizontally in a sample holder on top of a flexible pillar made of a 9 cm length of small diameter aluminum tubing. Mounted below the sample holder are four small coils of wire spaced at right angles in a plane normal to the pillar, only two of the four coils are shown in Fig. 1. Situated about each coil is a set of stationary Cobalt-Samarium magnets. The introduction of rare earth magnets has resulted in a significant increase in magnetic field density over earlier versions of the scanner.

Two of the coils, an orthogonal pair, are used to drive the flexible pillar and sample holder in two dimensions. The other coils are used to detect the velocity of the sample holder. The velocity signals are used in a servo loop to improve the mechanical response of the system and to reduce the effect of any external vibrations coupled into the scanner. Velocity signals are also integrated to give the position of the sample. The true position of the sample is always accurately known even in an environment where external vibrations couple into the mechanical system of the scanner. This position information is then used to control the electron beam of the CRT display (or scan converter) so that a true image is formed on the screen in synchronism with the position of the sample. The fast axis of the raster scan is usually driven at a 30 Hz rate. The time required to scan one frame is 10 to 30 seconds.

The top of the flexible pillar travels in an arc rather than a plane and the lens to sample spacing does change as a function of sample position. This effect is small, however, because the pillar is relatively long and the scanned field is generally less than 250 μm on a side. We reduce this effect still further with a piezoelectric element that is used to control the focal position of the lens in such a way as to compensate for non-planar motion of the sample.

With our present levels of external vibration the scanner deviates from an ideal raster pattern by only 2000 $\mathring{A}$. This deviation does not appear in the images since we can monitor the position of the sample with an uncertainty that is less than 1000 $\mathring{A}$. In liquid helium vibrations from the vacuum pump used to maintain the helium bath at 1.95°K degrade the scanner performance and image quality to some extent. We plan to correct this by further isolation of pump vibrations, by increasing the stiffness of the flexible pillar and by improving the scanner electronics and position sensors so that we can follow the motion of the sample with greater accuracy.

2. Operation in Liquid Argon and Nitrogen

A benchmark in our efforts to operate the acoustic microscope at cryogenic temperatures was established when we were able to operate in liquid argon at $85^{\circ}K$. This liquid was chosen as an intermediate point between water and liquid helium. It has acoustic properties similar to water except that its velocity is lower. We were, therefore, able to use the same sapphire lenses in both water and liquid argon. As in water, a single quarter wave matching layer of glass provided a good power match. In liquid argon the cryogenic microscope is operated at 2 GHz . At this frequency the wavelength in the liquid was 4300 $\mathring{A}$ - equal to wavelengths in the violet part of the optical spectrum. The high resolution of the argon microscope is demonstrated in Fig. 2.

Here a comparison is made between acoustic, scanning electron and optical micrographs of a grating.[2] The grating was made by exposing a 1500 $\mathring{A}$ layer of photoresist on a silicon wafer using two interfering optical beams. The photoresist lines are 2000 $\mathring{A}$ wide and the center-to-center spacing between lines is 4000 $\mathring{A}$. The acoustic microscope clearly resolves the lines and there is a considerable amount of detail on the line edges. The contrast is excellent. After viewing acoustically the sample was coated for viewing in the SEM (Fig. 2(b) to prevent charging effects. The acoustic image shows a surprising amount of surface detail when compared to the SEM image. Figure 2(c) shows the same object viewed with an optical microscope fitted with a high power, dry objective. The small change in index of refraction between air and photoresist was necessary to observe the sample after metalization to enhance contrast for optical viewing.

We have examined several other objects in the argon microscope, chosen from materials, integrated circuits, and biology. We were able to produce excellent

images of a spread of human metaphase chromosomes which are natural objects with submicron structures. Contrast with this object was high and resolution was at least as good as high quality oil immersion optical micrographs.

Figure 3 was chosen to illustrate performance with integrated circuits as objects. Here we have imaged a microwave dual gate field effect transistor (FET).[3] The two linear features are the gate electrodes which are 1 μm wide. Figures 3(a) and (b) are acoustic micrographs taken at two different focuses. Figure 3(c) is an optical image of the same device using a high power oil immersion objective.

Recently we have operated the cryogenic instrument in liquid nitrogen near $77^{\circ}K$. Based on the values for velocity and attenuation that we had at the time, we expected minimum wavelengths in nitrogen to be 15% larger than in argon.[4] In fact they turned out to be only 8% larger, as supported by more recent measurements by other groups.[5] Since nitrogen is a less expensive and more readily available liquid than argon, we will continue our studies with liquid nitrogen.

3. Liquid Helium

The most interesting liquid for cryogenic acoustic microscopy is liquid helium. At $1.95^{\circ}K$ it should be possible to build a microscope in helium using wavelengths three to four times shorter than those in water at room temperature. Several interesting projects, for example, imaging normal regions in type I and type II superconductors may be possible using the cryogenic microscope at these low temperatures.

Operation in liquid helium requires that we deal with problems that are not encountered with other liquids. The major problem is the low acoustic impedance of the liquid, $Z_{He} \sim .03 \times 10^5$ gm/cm^{2}sec as compared to the value of 1.5×10^5 for water.

At the interface between a solid and a liquid, the reflection coefficient for acoustic waves is large since there is a large difference in acoustic impedance between the two materials. For example, at the interface between sapphire and water, 13% of the power normally incident in a plane wave is transmitted. At a sapphire-helium boundary only 0.3% of the power is transmitted. Expressed in decibels the transmission coefficient is -25 dB .

A standard approach for solving a mismatch problem with coherent waves is to place one or more quarter wave matching layers between the solid and the liquid. We have pursued this course as a solution to the acoustic mismatch. Our problem is complicated in two ways. First, we operate at frequencies far above normal acoustic operating frequencies and our matching layers must be thin (~ 1 μm). These films are formed by vacuum deposition. This creates the second problem for there is only a limited class of materials that can be deposited with vacuum techniques. We must choose from this short list.

The ideal matching layer would have an acoustic impedance equal to the geometric mean of the values for the solid and the liquid helium. For fused quartz this ideal value is 0.7×10^5 gm/cm^2 sec. For sapphire it is 1.2×10^5 gm/cm^2 sec. A limited class of materials, mostly plastics, possess impedances near these values.

The range of materials can be extended by using a second quarter wave matching layer. The first layer is chosen to have a very high acoustic impedance. This effectively increases the impedance of the lens material and makes it possible to choose as a second layer a material of relatively high impedance. This combination will produce a reasonable match into liquid helium but the bandwidth will be narrower. We can compare the different combinations, with the following expression for the transmission coefficient. It is written in terms of the impedances of the lens

material (Z_s) , the first and second layers (Z_1 and Z_2) and the helium (Z_{He}) :[6]

$$T(dB) = 10 \log \left(\frac{4Z_{He}Z_2^2Z_s/Z_1^2}{\left(\frac{Z_2^2Z_s}{Z_1^2} + Z_{He}\right)^2} \right) \qquad (1)$$

This expression is valid for lossless, isotropic media at the quarter wave resonant frequency of the layers.[6] For a single layer $Z_1 = Z_s$ or $Z_2 = Z_{He}$.
In Table I we list a variety of possible matching schemes and compare their transmission efficiencies. We have experimented with several of these schemes and found three to show some promise. Preliminary experiments with a single quarter wave layer of carbon deposited by E-beam deposition[7] showed that satisfactory carbon films with good mechanical properties after cycling several times to low temperatures could be produced. The films were hard and exhibited low acoustic attenuation; however, the acoustic impedance was found to be about 8×10^5 gm/cm^2 sec, which provides a poor match to helium. Carbon should be useful in a double layer scheme. We also were successful in producing good quality polyethylene films with an acoustic impedance of about 3×10^5 gm/cm^2 sec. These films were found to have unacceptably high acoustic attenuation at room temperature. This may improve somewhat at low temperatures if thermal expansion effects do not damage the film. Finally we have produced a double quarter wave layer match of gold and glass which we used successfully in our initial helium microscope.

The properties of quarter wave matching layers for use in helium are initially evaluated using water at room temperature. Test "flats" were prepared by depositing ZnO transducers on one end of a short (1 mm) sapphire rod with the c-axis aligned along the rod axis. The ends of the rod were accurately parallel and carefully polished. The films to be evaluated were deposited on the opposite end.

Acoustic pulses centered at frequency f were generated in the rod and the echo train produced by the multiple reflections observed on an oscilloscope. The amplitude of a particular echo (normally the first) was measured with the rod in contact with air only (total reflection) and with a drop of water applied to the matching layers. The ratio of these amplitudes squared (or the difference in decibels) is the reflection coefficient of the test piece-water interface at the frequency f. Measurements at several frequencies near the quarter wave resonant frequency of the layers gives the frequency dependence of the reflection coefficient. For the case of a single layer the center frequency together with the measured thickness of the layer yields a value for the longitudinal velocity of sound in the layer, while the magnitude of the reflection coefficient gives the acoustic impedance. For two layers of thicknesses d_1 and d_2 the expected frequency dependence of the reflection coefficient $R(f)$ can be written in the same approximation as eq. (1) as[6]

$$R(f) = \left| \frac{Z - Z_\ell}{Z + Z_\ell} \right|^2 \qquad (2)$$

where $$Z = \frac{Z_s Z_1 - Z_s Z_2 \tan\phi_1 \tan\phi_2 - i(Z_1^2 \tan\phi_1 + Z_1 Z_2 \tan\phi_2)}{Z_1 Z_2 - Z_1^2 \tan\phi_1 \tan\phi_2 - i(Z_s Z_2 \tan\phi_2 + Z_s Z_1 \tan\phi_2)} \cdot Z_2$$

$$\phi_1 = \frac{2\pi f}{c_1} d_1$$

$$\phi_2 = \frac{2\pi f}{c_2} d_2$$

and c_1 and c_2 are the acoustic velocities in layers 1 and 2 respectively.

For two layers the impedance and velocity of the low impedance, outer layer are separately evaluated. Then eq. (2) with $Z_2 = Z_\ell$ can be inverted to obtain Z_1. From these measurements the expected transmission coefficient into liquid helium T(f) can be calculated using eq. (2) with $Z_\ell = Z_{He}$ and recalling that $T(f) = 1 - R(f)$.

The curves of Figs. 4 and 5 are data taken on glass and gold-glass matching devices. Figure 6 shows the predicted frequency dependence of the matching section in liquid helium. At the center frequency, the transmission coefficient to helium is nearly 10%. This can be improved upon using different materials as indicated in Table 1, but the gold-glass matching section was adequate for initial work at 630 MHz with the temperature held at $1.95^{o}K$. At this temperature and frequency the wavelength in liquid helium is 3600 $\mathring{A}$.

For our first object in liquid helium we chose a silicon on sapphire integrated circuit. Optical and acoustic micrographs are shown in Fig. 7. The vertical bar is aluminum and it is 1.0 μm thick. Successive acoustic micrographs were taken at slightly different focal positions. Figure 7(c) is the greatest lens to object spacing and represents focus on the top of the aluminum stripe. The image of Fig. 7(b) is slightly closer than the focus and (a) is still closer. Depth of field and phase effects are evident in (c) where only the thicker aluminum is visible. Due to the imperfect match (even with the layers most of the acoustic power is reflected at the sapphire-helium interface and remains in the crystal) the information pulse interfered with pulses in the sapphire rod produce the fringes and some of the contrast variations in the images. Such defects will be eliminated by improving the match. Even so features with sizes in the micron range are evident, especially edge roughness apparent in Fig. 7(a).

4. Conclusion

We plan in the coming year to improve the operation of the liquid helium microscope, chiefly through development of more efficient matching layers. We expect to reach frequencies near 1 GHz and wavelengths as small as 2000 $\mathring{A}$ in helium at $1.95^{o}K$. We also plan to apply the liquid helium microscope to several problems, especially studies in superconductors. Finally we will adapt the microscope for operation at temperatures below $0.5^{o}K$ in liquid helium, where we expect to be able to extend the resolution of the cryogenic scanning acoustic microscope. The absorption of acoustic waves at this temperature is lower than other liquids. This will allow us to work at higher frequencies. We will also be entering unknown territory for the physics of microwave sound propagation at these low temperatures has not been experimentally studied and it is not completely understood.

REFERENCES

1. "Acoustic Microscopy at Cryogenic Temperatures" - Annual Summary Report, G. L. Report No. 2865, September 1978.
2. Courtesy of IBM Corporation.
3. Courtesy of Hewlett-Packard Company.
4. M. Greenspan, "Acoustic Properties of Liquids" in A.I.P. Handbook, McGraw-Hill, New York (1973), third edition, from the measurements of J. Galt, J. Chem. Phys., 16, 505 (1948).
5. B. G. Dudar and S. A. Mikhailenko, Sov. Phys. Acoust. 22, 287 (1976). See also, A. E. Victor and R. T. Beyer, J. Chem. Phys. 52, 1573 (1970).
6. L. Brekhovskikh, Waves in Layered Media, Academic Press, New York (1960), Chapter 1.
7. Courtesy of A. Haubold, Gulf Atomic Corporation.

TABLE 1

Properties of Various Quarter Wave Matching Schemes

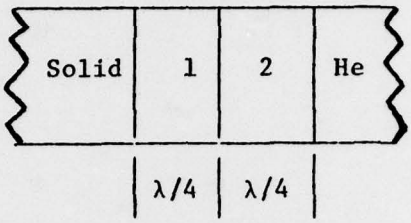

Lens Material	Layer 1	Layer 2	−T(dB)
Sapphire ($A\ell_2O_3$)	-	-	25
"	Glass	-	14
"	Carbon	-	6
"	Polyethylene	-	2
"	Au	Aℓ	14
"	Au	Glass	11
"	Au	Carbon	3*
"	W	Glass	7
"	W	Carbon	1*
Fused Quartz	-	-	20
"	Glass	-	19
"	Carbon	-	11
"	Polyethylene	-	4
"	Au	Aℓ	9
"	Au	Glass	5
"	Au	Carbon	2*

*Based on a value of impedance of 6×10^5 gm/cm^2 sec as found experimentally in low frequency measurements in a bulk sample of pyrolytic carbon.

FIGURE CAPTIONS

Fig. 1 Schematic of scanning stage used in cryogenic instrument.

Fig. 2 Photoresist grating, 4000 Å period - (a) acoustic; (b) SEM; (c) optical.

Fig. 3 Images of dual gate FET in liquid argon at about 85°K. Frequency is 2000 MHz. Gate width is about 1 μm.

Fig. 4 Frequency dependence of the reflection coefficient for a glass on sapphire to water match. Solid line is eq. (2) with $Z_2 = Z_\ell$, $Z_1 = 11.83 \times 10^5$ gm/cm^2 sec.

Fig. 5 Reflection coefficient for a gold-glass on sapphire to water match. Solid line is eq. (2) with $Z_1 = 57.55 \times 10^5$ gm/cm^2 sec, $Z_2 = 11.83 \times 10^5$ gm/cm^2 sec.

Fig. 6 Calculated transmission coefficient for gold-glass on sapphire to helium match. Layer impedances are the same as Fig. 5.

Fig. 7 Images in liquid helium at 2°K of an integrated circuit. Wavelength is 3600 Å.

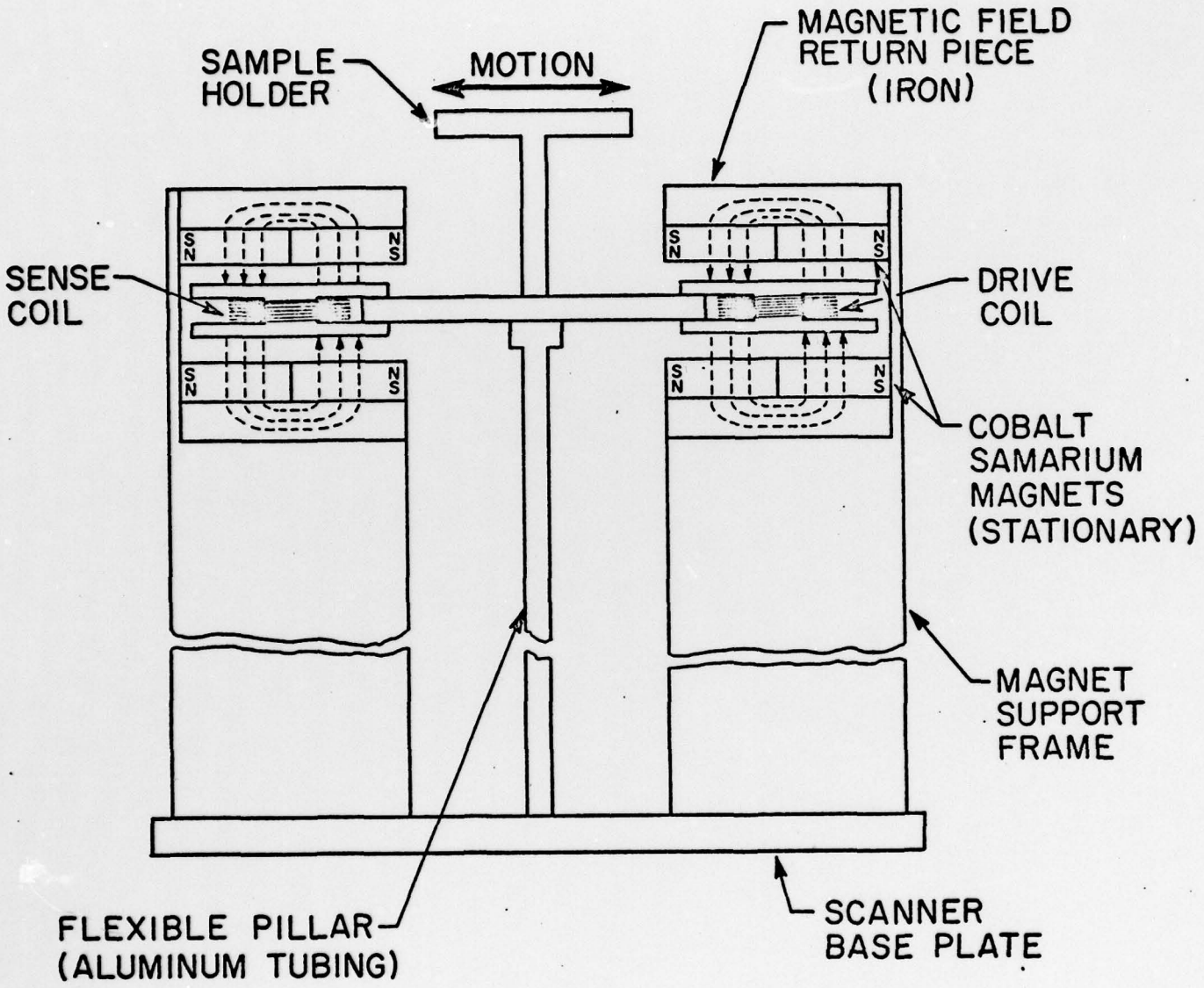
SAMPLE HOLDER
MOTION
MAGNETIC FIELD RETURN PIECE (IRON)
SENSE COIL
DRIVE COIL
COBALT SAMARIUM MAGNETS (STATIONARY)
MAGNET SUPPORT FRAME
FLEXIBLE PILLAR (ALUMINUM TUBING)
SCANNER BASE PLATE
S
N
N
S

FIGURE 1

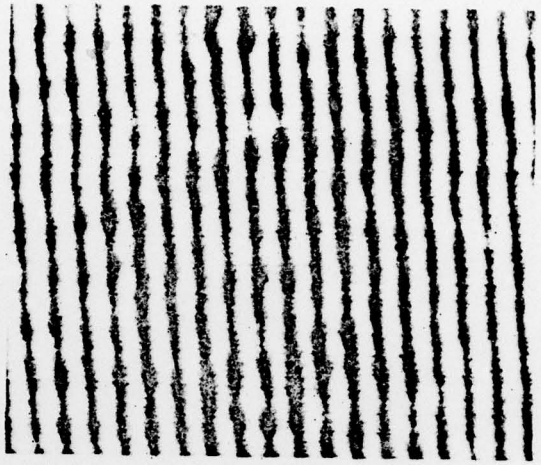

(a)

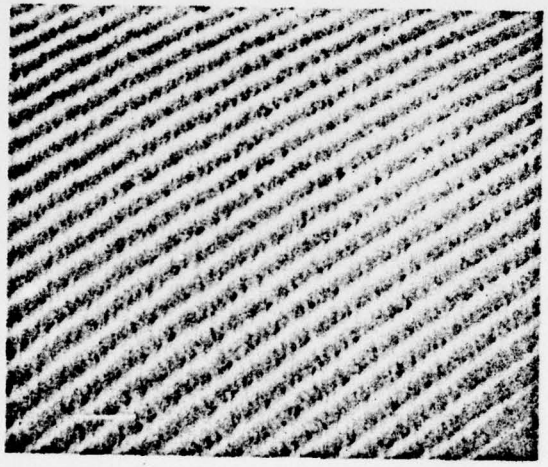

(b)

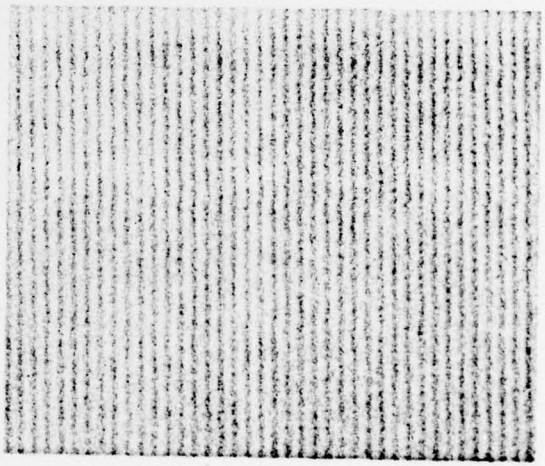

(c)

FIGURE 2

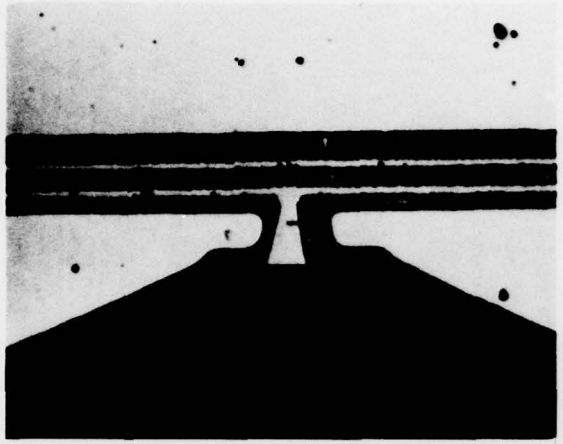

(a)

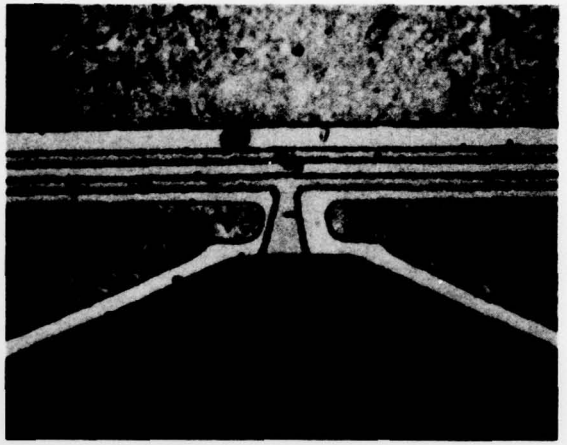

(b)

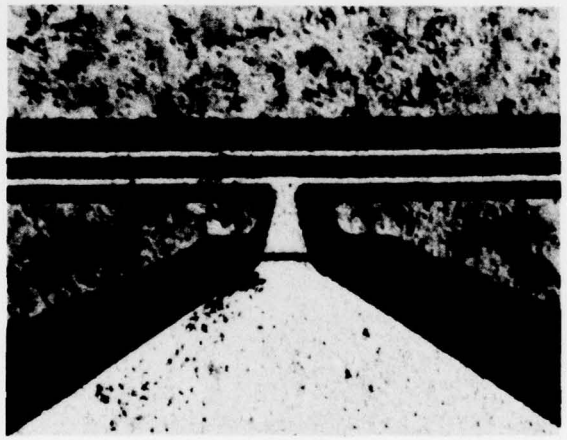

(c)

FIGURE 3

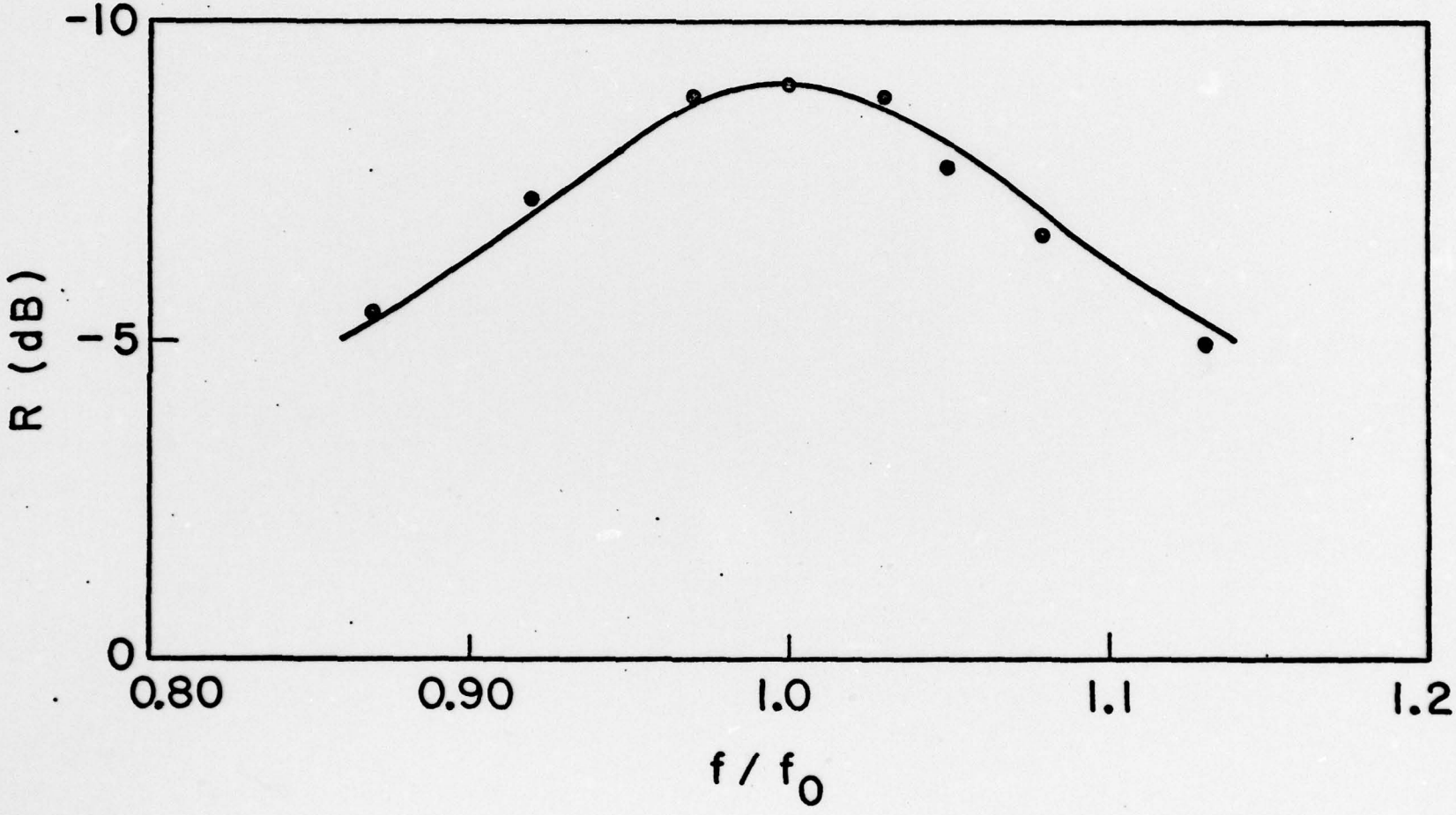

FIGURE 4

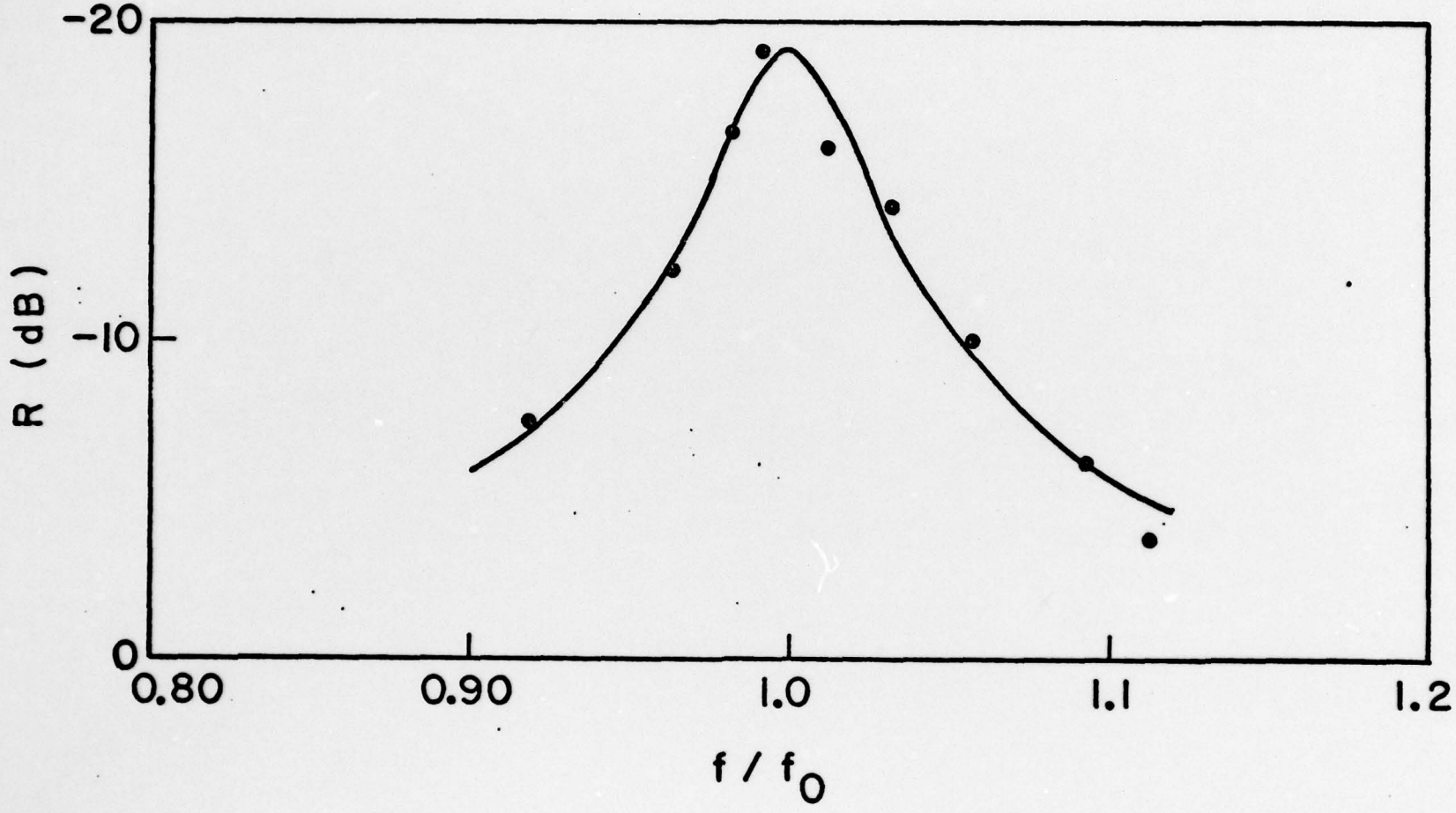

FIGURE 5

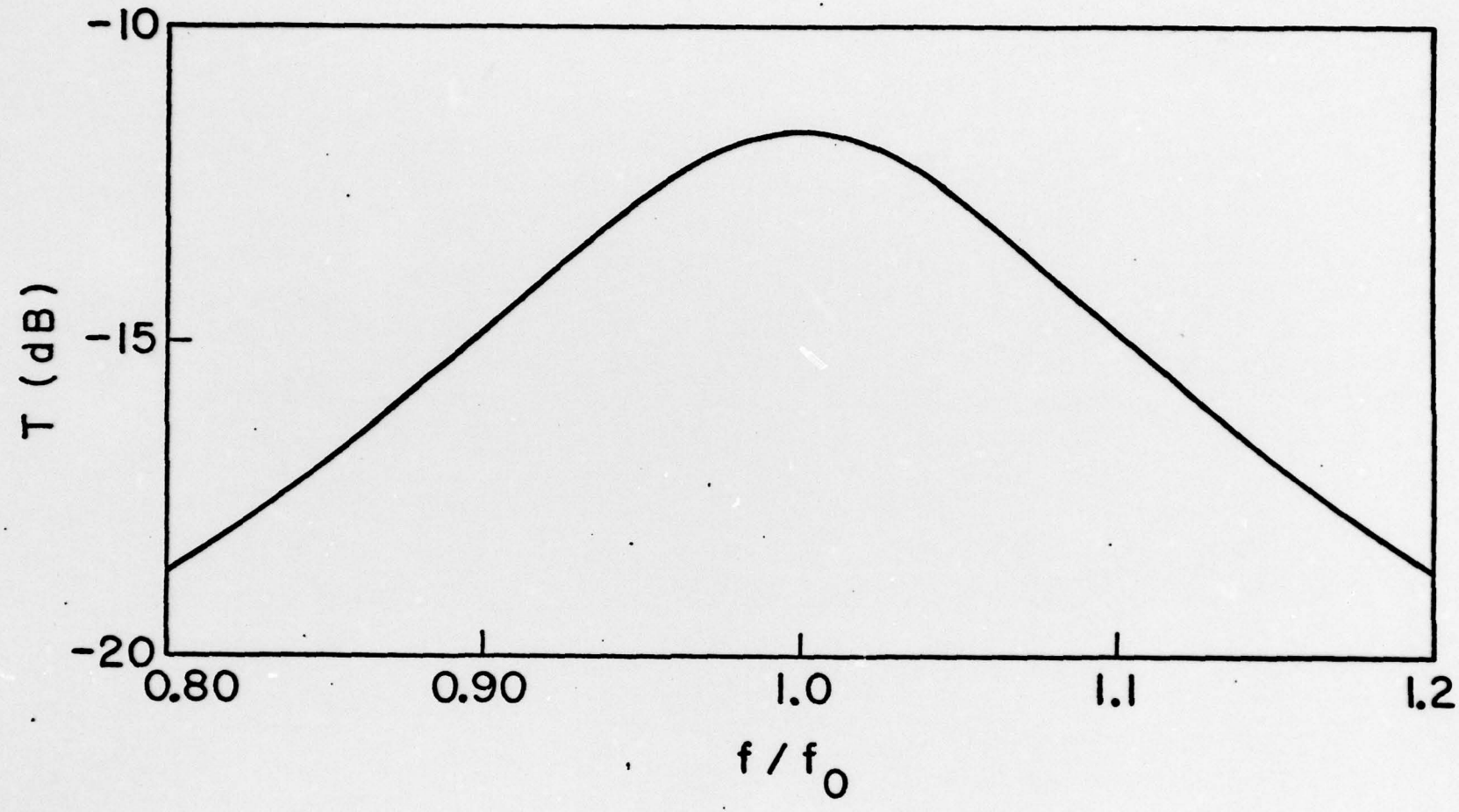

FIGURE 6

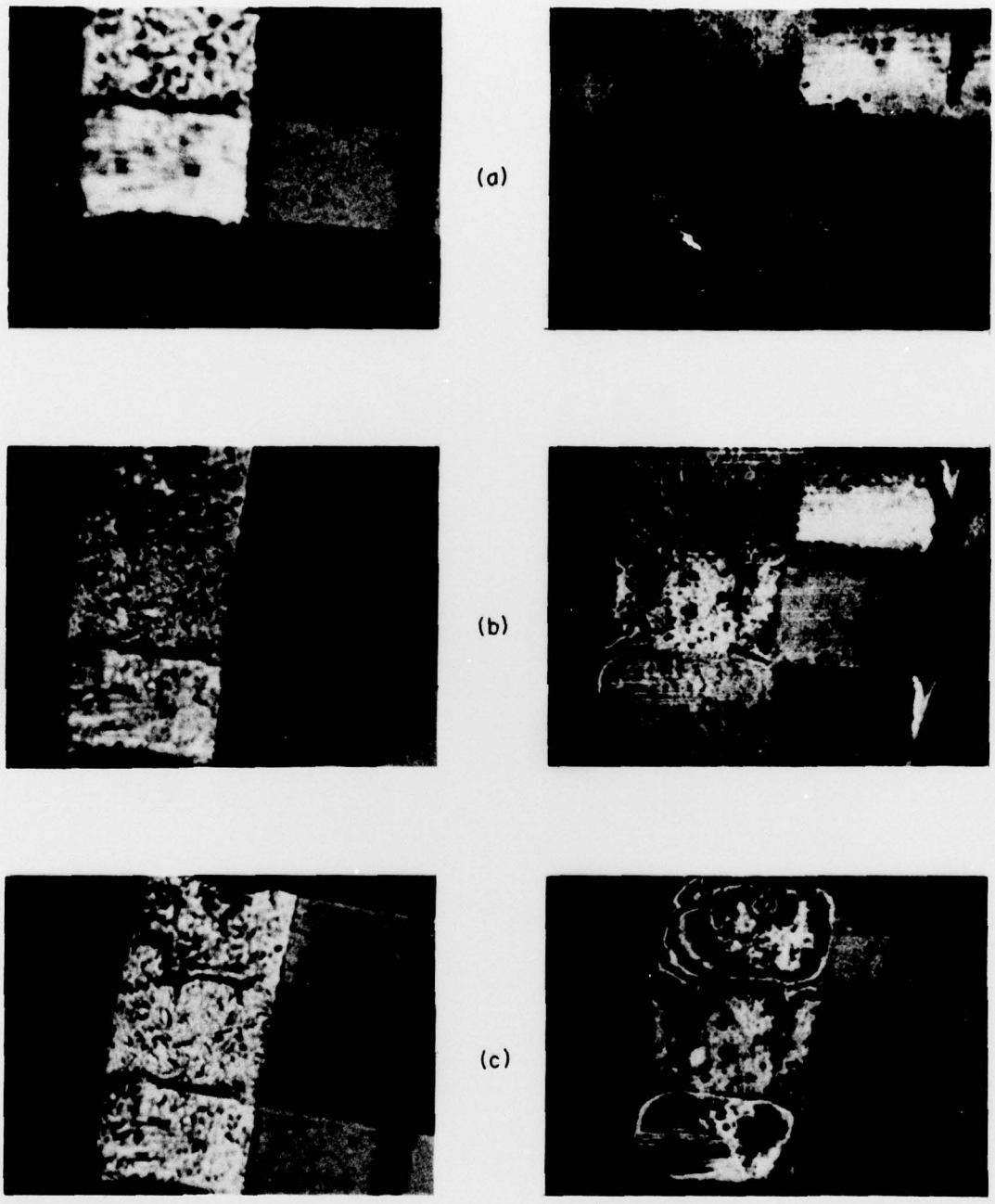

FIGURE 7